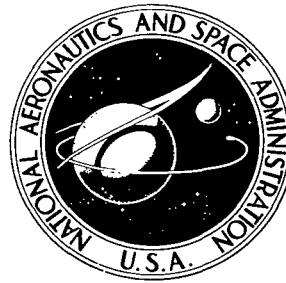


NASA TECHNICAL NOTE



NASA TN D-5837

C. I

NASA TN D-5837

ICAN COPY REPORT
A-15 (100)
KIRTLAND AFB, TX

0132592



**DAISY - AN EFFICIENT PROGRAM FOR
PRODUCTION OF NEUTRON PSEUDO
RESONANCE PARAMETER CHAINS IN
THE UNRESOLVED ENERGY REGION**

by Thor T. Semler

*Lewis Research Center
Cleveland, Ohio 44135*

NATIONAL AERONAUTICS AND SPACE ADMINISTRATION • WASHINGTON, D. C. • MAY 1970



0132592

1. Report No. NASA TN D-5837	2. Government Accession No.	3. Recipient's Catalog No.
4. Title and Subtitle DAISY - AN EFFICIENT PROGRAM FOR PRODUCTION OF NEUTRON PSEUDO RESONANCE PARAMETER CHAINS IN THE UNRESOLVED ENERGY REGION	5. Report Date May 1970	6. Performing Organization Code
7. Author(s) Thor T. Semler	8. Performing Organization Report No. E-5378	10. Work Unit No. 129-02
9. Performing Organization Name and Address Lewis Research Center National Aeronautics and Space Administration Cleveland, Ohio 44135	11. Contract or Grant No.	13. Type of Report and Period Covered Technical Note
12. Sponsoring Agency Name and Address National Aeronautics and Space Administration Washington, D. C. 20546	14. Sponsoring Agency Code	
15. Supplementary Notes		
16. Abstract A computer program for efficiently generating neutron pseudo resonance parameter chains is presented. The code DAISY makes use of the Central Limit Theorem to select chains that reproduce average cross section values. The code uses both the χ^2 and Kolmogorov-Smirnov tests for goodness of fit to produce chains of resonance parameters with the Porter-Thomas and Wigner distribution functions. As an example, the code is used to generate U^{238} cross sections in the unresolved resonance region near 20 keV. These continuous cross sections are used to calculate the Doppler effect, and to estimate the s-wave, p-wave overlap effects at 20 keV. The computed Doppler coefficient for U^{238} at 20 keV is consistent with other theoretical calculations for both a thin foil and a thick sphere.		
17. Key Words (Suggested by Author(s)) Pseudo resonance; Mock cross sections; Unresolved resonance; Uranium 238; Doppler effect; Cross section generation; Monte Carlo; Porter-Thomas distribution; Wigner distribution; Level spacing distribution; Level width distribution	18. Distribution Statement Unclassified - unlimited	
19. Security Classif. (of this report) Unclassified	20. Security Classif. (of this page) Unclassified	21. No. of Pages 43
		22. Price* \$3.00

CONTENTS

	Page
SUMMARY	1
INTRODUCTION	2
STOCHASTIC GENERATION OF RESONANCE PARAMETERS	3
Wigner Level Spacing Distribution	4
Level Width Distribution of Porter-Thomas	5
Sampling From the Normalized Wigner Distribution	6
Sampling From the χ^2 or Porter-Thomas Distribution	6
Central Limit Theorem	8
FINAL SELECTION OF BEST RESONANCE CHAIN	11
Kolmogorov-Smirnov Test	12
χ^2 Test for Goodness of Fit	13
Timing	14
CALCULATION OF U^{238} RESONANCE PARAMETERS NEAR 20 keV	15
RESULTS	16
Average Cross Section Calculations	16
Graphical Comparisons with Theoretical Distributions	21
ANALYSIS OF DOPPLER EFFECT EXPERIMENTS: CALCULATION OF HOT TO COLD CAPTURE RATIOS OF THE $U^{238} (n, \gamma) U^{239}$ REACTION AT 20 keV	21
Thin Foil Problem	21
Thick Sphere Problem	29
SUMMARY OF RESULTS	30
APPENDIXES	
A - SAMPLING FROM A χ^2 DISTRIBUTION	32
B - FAST GENERATOR FOR NORMAL RANDOM VARIABLES	35
REFERENCES	38

DAISY - AN EFFICIENT PROGRAM FOR PRODUCTION OF NEUTRON
PSEUDO RESONANCE PARAMETER CHAINS IN THE
UNRESOLVED ENERGY REGION

by Thor T. Semler
Lewis Research Center

SUMMARY

The code DAISY provides a fast technique for generating pseudo resonance parameters in the unresolved resonance region. The code makes use of the Central Limit Theorem in order to select chains of resonance parameters whose average values are inside a predetermined limit of accuracy. The Kolmogorov-Smirnov test for goodness of fit is used on chains of 5 through 100 resonances to determine the chain that best fits the Porter-Thomas and Wigner distribution functions. The χ^2 test for goodness of fit is used on chains of more than 100 resonances to determine that chain which best fits these distribution functions.

The code DAISY is found to be at least an order of magnitude faster than PSEUDO, a comparable code.

As an example, the code DAISY is used to compute s- and p-wave resonance parameters for U^{238} near 20 keV. From these parameters continuous cross sections are computed and used to calculate the Doppler effect in a 0.0155-centimeter-thick U^{238} foil and in a 2-centimeter-diameter U^{238} sphere, at 20 keV.

It is found that using the set of pseudo resonance parameters chosen by DAISY, one may preserve the measured value of the total cross section, and the Doppler effects so computed, are compatible with other theoretical computations of the Doppler effect. It is also found that, while the average s-wave capture cross section at 20 keV is about one-third that of the p-wave, the s-wave contribution to the Doppler effect is about 60 percent. The effect of neglecting resonance series overlap is to overestimate the Doppler effect.

INTRODUCTION

Continuous neutron cross sections in the unresolved energy region are needed to calculate fast neutron Doppler effects, to analyze fast neutron transmission experiments, and to estimate stellar reaction rates. The unresolved resonance region generally spans an energy region from about 1 keV to about 1 MeV. In figure 1 the neutron capture cross

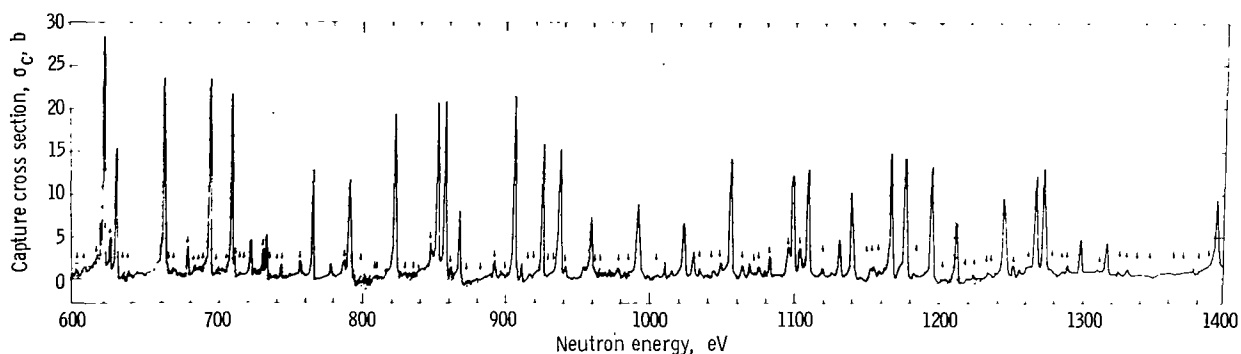


Figure 1. - Portion of experimental capture data from first U^{238} sample in neutron beam from Petrel event. Small arrows indicate locations of weak resonances which are assigned $l = 1$. Data from more sensitive detectors and thick sample were used in confirmation and measurement of these resonances.

section of uranium-238 (U^{238}) is shown in a part of the resolved resonance region (ref. 1). In figure 2 the neutron capture cross section of U^{238} is shown for the unresolved resonance region (ref. 2). Figure 2 depicts the results of 16 different experiments that differ by as much as 40 percent. The results of figure 2 are averages over several resonances.

Various analytic approaches have been adopted to calculate average cross sections in the unresolved region. In an attempt to evaluate fission product reactivity effects, in intermediate reactors, a method using strength function data was developed (refs. 3 to 5). However, this statistical averaging method does not provide the detailed energy dependent cross sections necessary for the calculation of a fast reactor Doppler effect.

If it is assumed that the statistical distributions of resonance parameters found at low neutron energies are obeyed at the higher unresolved energies, it is possible to sample from these distributions and generate "pseudo" or "mock" resonance parameters. These pseudo resonance parameters have been used to compute energy dependent cross sections with correct average properties (refs. 6 to 10). Brissenden and Durston have used sampling techniques to generate sets of mock cross sections for U^{238} (ref. 6).

In a series of experiments designed to measure the Doppler effect in U^{238} , Perkin

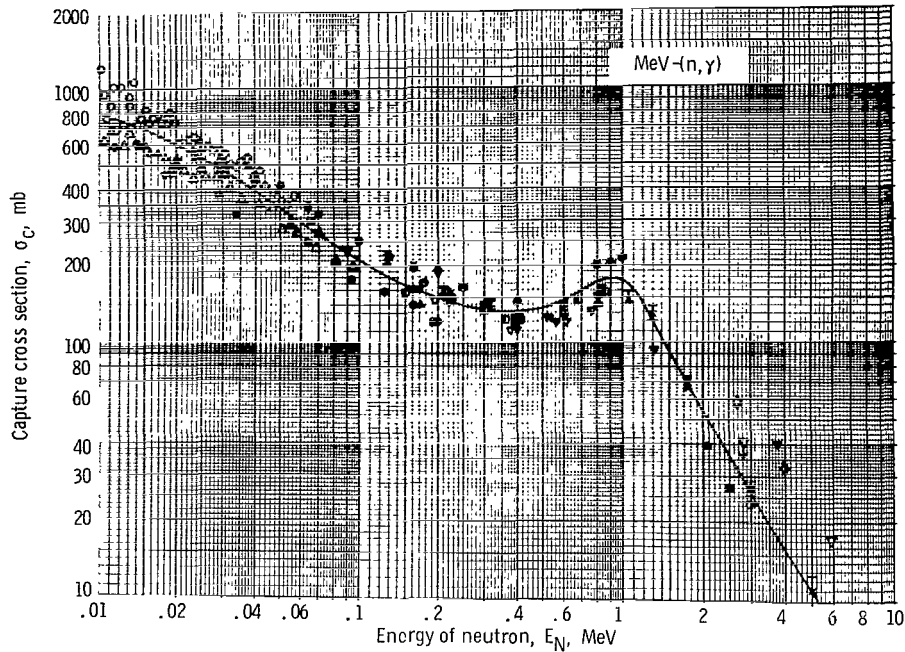


Figure 2. - Portion of unresolved resonance region for captures.

and Fieldhouse used a modification of the method of Brissenden and Durston to compute the Doppler effect theoretically (refs. 11 and 12). However, the computer time necessary to generate these mock cross sections is prohibitively large, ~ 2.5 hours per isotope per temperature on an IBM-STRETCH computer.

The code DAISY described herein is one to two orders of magnitude faster in the generation of resonance parameters than the code PSEUDO (ref. 9) which has a timing of about 139 resonances per second on the UNIVAC 1108. DAISY also allows substantial flexibility, in that, short resonance chains, as few as five resonances in a chain, can be generated.

In order to illustrate the versatility of the code DAISY, it is used with the code GAROL (ref. 13) to analyze the effect of s- and p-wave resonance series overlap. The method is applied to compute the Doppler effect for a 0.0155-centimeter slab of U^{238} and a 2.0-centimeter sphere of U^{238} at 20 keV (refs. 12 and 14).

STOCHASTIC GENERATION OF RESONANCE PARAMETERS

In order to generate neutron resonance cross sections, one needs the resonance parameters associated with the Breit-Wigner single-level formula. These are the energy

of the resonance E_0 , the scattering width of the resonance Γ_n , and the capture width of the resonance Γ_γ .

These measured parameters allow one to compute accurate values of the continuous neutron cross sections from resonance to resonance (ref. 13).

It has been asserted on the basis of theoretical considerations that these resonance parameters have definite analytic probability distributions (refs. 15 to 17). The level spacing distribution of Wigner and level width distribution of Porter and Thomas have been checked experimentally in the resolved resonance region for many isotopes, and they have been found to adequately describe the distributions of parameters measured experimentally (refs. 18 to 20).

One may assume that the statistical distributions found to obtain at low neutron energies are also valid for higher neutron energies. Thus one may employ these distributions of resonance parameters to generate a set of pseudo resonance parameters in the unresolved resonance region. The code DAISY described below allows one to generate chains of pseudo resonance parameters, in the unresolved resonance region, which preserve the correct average values, as well as, an accurate representation of the correct distribution functions.

Wigner Level Spacing Distribution

It is found that the level spacing between two neutron resonances, of like J and l , follows a probability distribution of the form

$$p(x) = \frac{\pi}{2} x \exp\left(\frac{-\pi}{4} x^2\right) \quad x \geq 0$$

$$p(x) = 0 \quad x < 0 \tag{1}$$

where J is the spin quantum number of the compound nucleus formed by the target and the neutron, l is the angular momentum of the neutron with respect to the target nucleus, and x is a normalized dimensionless level spacing or

$$x = \frac{S}{\bar{D}_J} \tag{2}$$

where S is the nearest neighbor level spacing in eV and \bar{D}_J is the J state average level spacing in eV. Equation (1) is then the Wigner level spacing distribution (refs. 16 and 17).

Level Width Distribution of Porter-Thomas

The variation of the reduced scattering widths Γ_n^0 is found to follow a χ^2 distribution function (ref. 18) with one degree of freedom for s-wave ($l = 0$) resonances while two degrees of freedom have been suggested for p-wave ($l = 1$) resonances (ref. 15); that is,

$$\Gamma_n^0 = E_0^{-1/2} \nu_l^{-1} \Gamma_n \quad (3)$$

where E_0 is the resonance energy in eV, ν_l is the penetrability factor, and Γ_n is the scattering width associated with the Breit-Wigner formula. The distribution of

$$y = \frac{\Gamma_n^0}{\Gamma_n^0} \quad (4)$$

is found to be of the form

$$\left. \begin{aligned} p(y, \nu) &= \left[2^{\nu/2} \Gamma\left(\frac{\nu}{2}\right) \right]^{-1} y^{(\nu/2)-1} e^{-y/2} & y \geq 0 \\ p(y, \nu) &= 0 & y < 0 \end{aligned} \right\} \quad (5)$$

where the number of degrees of freedom ν is equal to 1 for s-wave resonances and equal to 2 for p-wave resonances. This is the distribution of Porter and Thomas for scattering widths.

The capture width Γ_γ is found to vary little from resonance to resonance. This, in fact, is consistent with the theory of Porter and Thomas which indicates Γ_γ should be distributed as χ^2 with a large number of degrees of freedom (ref. 21). Since the mean square deviation about the mean for a normalized χ^2 distribution is two over the number of degrees of freedom, Γ_γ should remain relatively constant from resonance to resonance. However, some recent experiments tend to cast doubt on the assumption of a constant Γ_γ (refs. 1 and 22).

If these distributions are assumed to be valid for higher neutron energies, one may sample from the Wigner level spacing distribution to obtain a series of E_0 's and then sample from a χ^2 distribution (Porter-Thomas) for the corresponding Γ_n 's. This technique may be used to generate continuous cross sections in the energy region between the highest measured resonance and the energy region where the Doppler width becomes larger than the level spacing.

Sampling From the Normalized Wigner Distribution

When the Wigner level spacing distribution is written as equation (1), the \bar{D}_J multiplier has been normalized out. The expectation value of x , or the mean of x , is 1. It is adequate, for the present, to discuss the sampling from this normalized probability function. In order to sample X , a level spacing, from the normalized Wigner distribution (eq. (1)), one forms the functional mapping (eq. (6))

$$R_n = \int_{-\infty}^X p(x) dx \quad (6)$$

where R_n is a random number uniformly distributed on the interval (0, 1)

$$R_n = \frac{\pi}{2} \int_0^X x \exp\left(-\frac{\pi}{4} x^2\right) dx \quad (7)$$

Solving the previous equation for X gives

$$X = \frac{2}{\sqrt{\pi}} \sqrt{-\ln(1 - R_n)} \quad (8)$$

or since $1 - R_n$ is distributed as R_n

$$X = \frac{2}{\sqrt{\pi}} \sqrt{-\ln(R_n)} \quad (9)$$

One may now easily gain the correct J state level spacing by multiplying X by \bar{D}_J , the J state average level spacing.

Sampling From the χ^2 or Porter-Thomas Distribution

The Porter-Thomas or neutron width distributions can likewise be written in a normalized form

$$p(y, 1) = \left[2^{1/2} \left(\Gamma \frac{1}{2} \right) \right]^{-1} y^{-1/2} e^{-y/2} \quad (\text{s-wave}) \quad (10)$$

$$p(y, 2) = [2\Gamma(1)]^{-1} 2^{-1} e^{-y/2} \quad (\text{p-wave}) \quad (11)$$

where y is given by equation (4). It can be shown (see appendix A) that the problem of sampling a member from a χ^2 distribution with ν degrees of freedom can be reduced to the problem of sampling ν random values selected from a normal distribution of mean 0 and variance 1. That is, if the sequence

$$Y_1, Y_2, Y_3, \dots, Y_n, \dots$$

is composed of values selected from a normal distribution of unit variance and mean 0, the sequence of transformed random variables

$$Y_1^2, Y_2^2, Y_3^2, \dots, Y_n^2, \dots$$

has a χ^2 distribution with one degree of freedom and the sequence

$$(Y_1^2 + Y_2^2), (Y_3^2 + Y_4^2), \dots, (Y_{2n-1}^2 + Y_{2n}^2), \dots$$

has a χ^2 distribution with two degrees of freedom. However, each element of the second sequence must be divided by two in order to preserve normalized property. There are available many techniques for sampling from the normal distribution. A fast algorithm with a correct treatment of the wings of the normal distribution has been chosen (ref. 23). It is described in appendix B.

Once a series of E_0 's or resonance energies have been generated, one can sample from the appropriate χ^2 distribution; the value of Γ_n associated with an E_0 is then

$$\Gamma_n = E_0^{1/2} \nu_0 \bar{\Gamma}_n^0 Y_n^2 \quad (\text{s-wave}) \quad (12)$$

or

$$\Gamma_n = E_0^{1/2} \nu_1 \bar{\Gamma}_n^0 (Y_{2n-1}^2 + Y_{2n}^2) 2^{-1} \quad (\text{p-wave}) \quad (13)$$

where ν_0 and ν_1 are the penetrability factors,

$$\nu_0 = 1 \quad (\text{s-wave}) \quad (14)$$

$$\nu_1 = \frac{k^2 R^2}{1 + k^2 R^2} \quad (\text{p-wave}) \quad (15)$$

R is the nuclear radius and k is 2π times the wave number of the incident neutron (ref. 24).

Although it is possible to produce such resonance chains at will, a question arises as to how one might compare one such chain to another. Of course, given the same set of initial average resonance parameters, one will generate a somewhat different chain each time a chain is generated, depending upon the sampling method. For example, given a different random number generator for sampling purposes, one might use the same technique twice and obtain different results. Stated more accurately, given n such generated chains of m resonances, which of the n chains should be chosen as a representation of the actual resonance structure in this energy region? This difficulty has sometimes been rejected, by asserting, that since one was sampling correctly from the distributions, one chain of resonance parameters, so generated, was as good as any other such chain (ref. 6, pp. 75-76). Alternatively, an integral approach has been taken (ref. 9). In one such integral approach, several resonance chains are calculated, the (dilute resonance) integral of each chain is computed, and a chain with a resonance integral near the mean of these values is chosen as the best chain.

A different approach has been adopted herein, which gives not only the correct resonance integral value but also provides a much faster running time - comparable with single chain times. The present method for the choice of the best chain depends upon the use of the Central Limit Theorem, and on two statistical techniques for goodness of fit that are discussed separately. One technique has been devised for very short chains of resonances, 5 to 100 spacings. The other technique is applied to longer chains of 101 to 5000 spacings.

Central Limit Theorem

The expectation value of a sum is the sum of the expectation values, that is, if g_1, g_2, \dots, g_n are any random variables which have expectation values, then

$$E(g_1 + g_2 + \dots + g_n) = E(g_1) + E(g_2) + \dots + E(g_n) \quad (16)$$

If each of g_i are independently sampled from the same distribution, then the following relation results:

$$E(g_1 + g_2 + \dots + g_n) = nE(g_1) = nE(g_2) = \dots = nE(g_n) \quad (17)$$

Also if g_1, g_2, \dots, g_n are independent random variables, the variance of the sum is equal to the sum of the variances. That is,

$$\sigma_{g_1+g_2+\dots+g_n}^2 = \sigma_{g_1}^2 + \sigma_{g_2}^2 + \dots + \sigma_{g_n}^2 \quad (18)$$

Again, if each of the g_i are independently sampled from the same distribution,

$$\sigma_{g_1+g_2+\dots+g_n}^2 = n\sigma_{g_1}^2 = n\sigma_{g_2}^2 = \dots = n\sigma_{g_n}^2 \quad (19)$$

The Central Limit Theorem (refs. 27 and 30) states that, if g_1, g_2, \dots, g_n are random variables independently chosen from the same distribution each with expectation μ and variance σ^2 , then the probability distribution of the sum

$$S_n = g_1 + g_2 + \dots + g_n \quad (20)$$

is asymptotically normal as $n \rightarrow \infty$ or

$$\lim_{n \rightarrow \infty} P\left(\frac{S_n - n\mu}{\sigma\sqrt{n}} \leq w\right) = \frac{1}{\sqrt{2\pi}} \int_{-\infty}^w e^{-t^2/2} dt \equiv N(w) \quad (21)$$

It is found empirically that this limiting distribution, the standard normal distribution is assumed very rapidly for X_i 's chosen from the Wigner distribution. In fact, for n as small as 5, the distribution of the sums of X_i 's chosen from the Wigner distribution provide a good approximation to the standardized normal distribution. Thus one can compute both the probability, that the sum of n samplings from the Wigner distribution will be below a value S_- as well as the probability that the sum of n samplings will be above some value S_+ . This calculation allows one to select a probability level, say 85 percent, and to reject a chain immediately if it does not approximate the average level spacing better than 85 percent of such chains. At this point, it is useful to work through an example of such limits. The initial conditions are that

$$E_{\text{initial}} = 4500 \text{ eV}$$

$$E_{\text{final}} = 5000 \text{ eV}$$

$$\bar{D}_J = 5 \text{ eV}$$

Since

$$\frac{E_{\text{final}} - E_{\text{initial}}}{\bar{D}_J} = 100$$

the distribution function of the sum of 100 samplings and its variance from the normalized Wigner distribution is evaluated. It is well known that the variance is the expectation of the square of the difference between the mean and the random variable or

$$\sigma^2 = E[(X - \mu)^2] \quad (23)$$

$$\sigma^2 = E(X^2) - \mu^2 \quad (24)$$

Thus for the normalized Wigner distribution

$$\sigma^2 = \int_0^\infty x^2 p(x) dx - 1^2 \quad (25)$$

$$\sigma^2 = \int_0^\infty x^2 \frac{\pi}{2} x \exp\left(-\frac{\pi}{4} x^2\right) dx - 1 \quad (26)$$

$$\sigma^2 = \frac{4}{\pi} - 1 = 0.273239 \dots \quad (27)$$

$$\sigma = 0.5227232 \quad (28)$$

One can now generate the standard normal distribution, which very closely approximates the distribution of the sum of 100 random variables S_{100} sampled from the Wigner distribution after the form of equation (21); that is,

$$P\left(\frac{S_{100} - 100 \times 1}{0.5227 \sqrt{100}} \leq w\right) \doteq N(w)$$

$$P\left(\frac{S_{100} - 100}{5.227} \leq w\right) \doteq N(w)$$

One can now answer such questions as what is the probability that the sum S_{100} is between 99 and 101; that is,

$$S\left(\frac{99 - 100}{5.227} \leq -0.19\right) = N(-0.19) = 0.4247$$

$$P\left(\frac{101 - 100}{5.227} \leq 0.19\right) = N(0.19) = 0.5753$$

$$P(99 \leq S_{100} \leq 101) = 0.5753 - 0.4247 = 0.1506$$

If, for example, a probability level of 85 percent had been chosen for a chain of 100 levels, any chain adding up to less than 99 or more than 101 could be ignored. More detailed calculations could then be used to choose the best chain from the 15 percent accepted by this technique. Also, since the normal distribution is a symmetric function about the expected value of the sum, no bias has been introduced.

A similar technique is used for the scattering widths. Since the level widths are distributed as χ^2 , and as χ^2 does not approximate a normal distribution until many degrees of freedom are introduced, the sampling limits are chosen from the appropriate χ^2 distribution. Again the expectation of the sum is equal to the sum of the expectations. The sampling limits are adjusted such that no bias is introduced; (i. e., equal probability about the expected value). For an example similar to the aforementioned, the expected value of the sum of 100 values of $\chi_{\nu=1}^2$ is 100 and the 85 percent limits - 15 percent acceptance - are 97.375 and 102.715. The unequal spacing about 100 of the limits is such that no bias is introduced into the accepted values (ref. 26).

The aforementioned technique allows one to generate many resonance chains, all drawn from the correct sampling distributions, and to immediately reject those chains which are found to vary from the average by more than the limits set. No extensive calculations are wasted on these rejected chains. The values of both \bar{D}_J and $\bar{\Gamma}_n^0$ are preserved to within set limits. In the next section two techniques will be outlined which allow one to choose from the accepted chains, that chain, which best fits the distribution functions for D and Γ_n .

FINAL SELECTION OF BEST RESONANCE CHAIN

In the preceding section it was shown how one can reject resonance chains prior to any involved or detailed considerations on strictly statistical grounds. Two methods

which allow one to choose, from chains found acceptable by the above test, the "best" chain, in the sense of goodness of fit, are now described. The method found applicable to short chains (where n , the number of resonances, is less than or equal to 100 but greater than or equal to 5) was the Kolmogorov-Smirnov statistic for goodness of fit.

Kolmogorov-Smirnov Test

The cumulative distribution function $F(x)$ (eq. (29)) equals the probability that the random variable has some value less than or equal to x ; that is,

$$F(x) = \int_{-\infty}^x p(x)dx \quad (29)$$

If one also forms the discrete cumulative distribution function $F_n(x)$ for n samples from the distribution function, one can compute the Kolmogorov-Smirnov statistic Δ (ref. 27) as

$$\Delta = \text{least upper bound of } |F_n(x) - F(x)| \quad -\infty \leq x \leq \infty \quad (30)$$

The meaning of this statistic is illustrated in figure 3. Once one has computed Δ for each acceptable chain, that chain with Δ a minimum is chosen as the "best" chain. It can be seen that the minimum Kolmogorov-Smirnov statistic corresponds to the best

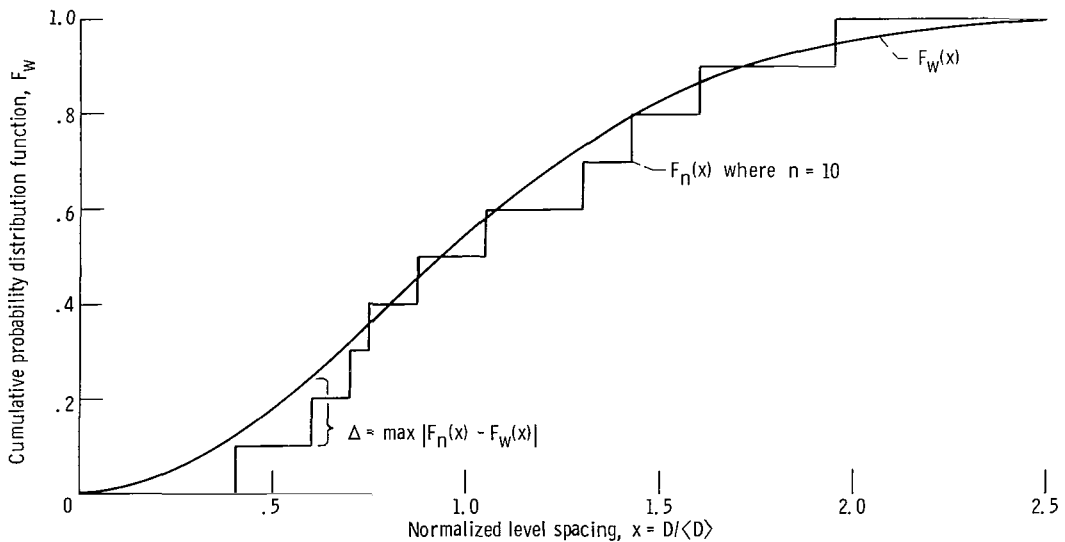


Figure 3. - Illustration of Kolmogorov-Smirnov test for goodness of fit.

fitting of the continuum distribution function by a discrete function. Thus by the introduction of the Central Limit Theorem the measured mean values of the level spacing and the scattering width are conserved, and by use of the minimum Kolmogorov-Smirnov statistic a very good fit to the distribution function is obtained. Hence, all the information available to the construction of the "best" chain has been applied. This method is quite fast for chains of n resonances where $5 \leq n \leq 100$.

For chains containing more than 100 resonances, a different technique has been employed in order to facilitate the choice of the "best" chain. The method which was adopted for the longer chains is the χ^2 test for goodness of fit.

χ^2 Test for Goodness of Fit

Due to the necessity of sorting individual values to compute $F_n(x)$ for the aforementioned Kolmogorov-Smirnov test, it is not particularly well suited to the production of long resonance chains. Again, however, we should like to maintain the correct distribution function. The technique best suited to such a requirement for large samples is the χ^2 test for goodness of fit. For this particular application, it has been implemented in the following manner. The probability distribution has been divided into 20 equally probable portions. Twenty were chosen in order to maintain an expected value in each portion, or bin, of more than five (ref. 28). Once a chain has been accepted by the Central Limit Theorem, the random variables used to generate it are placed in the appropriate bin corresponding to the 20 equally probable ones. Finally, when all the random variables have been tallied, the expected value for each bin is subtracted from the number actually found. The twenty values so generated are squared and summed. This sum is then divided by twenty and multiplied by the number of resonances. The resultant number is called the χ^2 of the fit and is a measure of the goodness of fit. If χ^2 is large, the fit to the distribution is poor; likewise, if χ^2 is small, the fit is good. Hence, the chain with minimum χ^2 is chosen as the best fit to the distribution function. This χ^2 is a number and is not to be confused with the distribution function of χ^2 which was discussed earlier in this report. The connection of this number and the distribution function is discussed in most books on statistical methods (refs. 29, 30, 25, and 28). Hence, the DAISY program by the use of rather simple and fast techniques has chosen the resonance chain which has an average level spacing and average reduced scattering width which are inside predetermined limits. DAISY has also chosen that chain whose elements best fit the two distribution functions associated with level width and level spacing.

Figure 4 shows the mechanics of the code DAISY in block diagram form.

per second on the IBM 7094-II. This may be compared with the timing of the PSEUDO code (ref. 9) which generates 1248 resonances in 9 seconds on the UNIVAC 1108 or about 138.7 resonances per second. Since the UNIVAC 1108 has a cycle time of about 0.75 microsecond and the 7094-II has a cycle time of about 1.4 microsecond, one may make a rather crude comparison of the two machines by the ratio of cycle times. If this is done for the PSEUDO code, one obtains a value of about 74.2 resonances per second on the IBM 7094-II. On the basis of this admittedly crude comparison, the DAISY technique is at least, since p-wave calculations are longer, 18.4 times faster than the technique of PSEUDO.

In comparing problem size limitations the maximum number of chains for DAISY is 9999, and the maximum number of ladders for PSEUDO is 500. The maximum number of resonances per chain in DAISY is 5000, and the maximum number of resonances per ladder for PSEUDO is 4000.

CALCULATION OF U^{238} RESONANCE PARAMETERS NEAR 20 keV

The use of the DAISY code for the generation of resonance parameters is illustrated for U^{238} . U^{238} has both zero spin and relatively well measured s- and p-wave strength functions (refs. 1, 20, 31 to 34). The zero spin property allows one to sample from a single Wigner level spacing distribution for s-wave resonances. The neutron energy region about 20 keV was chosen since the contribution of the p-wave component to the $U^{238}(n, \gamma)U^{239}$ cross section is near its maximum and should allow a convenient check on both the s- and p-wave components of the cross section averages.

To provide a set of resonance parameters suitable for further calculations, the following procedure is used:

(1) Using the strength functions and the average level spacing, $\bar{\Gamma}_n^0$ (s-wave) and $\bar{\Gamma}_n^0$ (p-wave) are determined.

(2) Within the energy limits, E_{initial} to E_{final} , the sets of resonance parameters Γ_n (s-wave) and E_0 (s-wave) are generated by DAISY for the best chain ($I = 0$) or chains ($I \neq 0$).

(3) The measured value of σ_{pot} and the values of $\bar{\Gamma}_n^0$ (p-wave) and \bar{D}_J (p-wave) are used to generate the sets of resonance parameters Γ_n (p-wave) and E_0 (p-wave) in this energy region for the best chain (unseparated spin statistics) or chains (separated p-wave spin statistics).

(4) Using the resonance parameters just generated and σ_{pot} (measured), average partial cross sections are computed for the range E_{initial} to E_{final} .

(5) The sum of the average partial cross sections

$$\bar{\sigma}_{\text{tot}}(\text{computed}) = \bar{\sigma}_{c_s} + \bar{\sigma}_{c_p} + \bar{\sigma}_{s_s} + \bar{\sigma}_{s_p} + \sigma_{\text{pot}}(\text{measured})$$

is compared with $\bar{\sigma}_{\text{tot}}(\text{measured})$ in this energy region.

(6) If necessary, the measured value of σ_{pot} is adjusted such that $\bar{\sigma}_{\text{tot}}(\text{measured})$ equals $\bar{\sigma}_{\text{tot}}(\text{computed})$.

(7) The final set of resonance parameters (p-wave parameters must be changed due to eq. (15)) will match the average total cross section and will have the specified average parameter values within the set limits.

RESULTS

Average Cross Section Calculations

As a test of the technique used in DAISY, the average partial cross section of U^{238} are calculated by the code GAROL (ref. 13). The GAROL code assumes a lattice of absorber lumps embedded in a moderating medium. It solves two coupled integral equations for the fluxes in each region. It also allows one to compute Doppler broadened cross sections directly from the Breit-Wigner resonance parameters provided by DAISY. A hydrogen-like ($A = 1.0$) pure scatterer has been chosen for the moderating material. A narrow energy region, 19.5 to 20.5 keV, has been chosen.

DAISY is used to generate s- and p-wave resonance parameters from 19.5 to 20.5 keV. The information used by DAISY is shown in table I. The p-wave parameters have been generated in this energy region using a measured value of σ_{pot} equal to 10.8 barns (ref. 35). The p-wave parameters have been chosen as merged, no J dependence, as there is no measured data on separated spin statistics for the p-wave resonances of U^{238} .

TABLE I. - PARAMETERS USED IN DAISY FOR U^{238}

Parameters	s-Wave	p-Wave
Angular momentum of neutron with respect to target nucleus, l	0	1
Capture width, Γ_{γ} , meV	23.8	23.8
Average reduced scattering width, $\bar{\Gamma}_n^0$, meV	1.83	3.7
Average level spacing, \bar{D} , eV	20.8	7.0
Potential scattering cross section, σ_{pot} , b	10.8	---

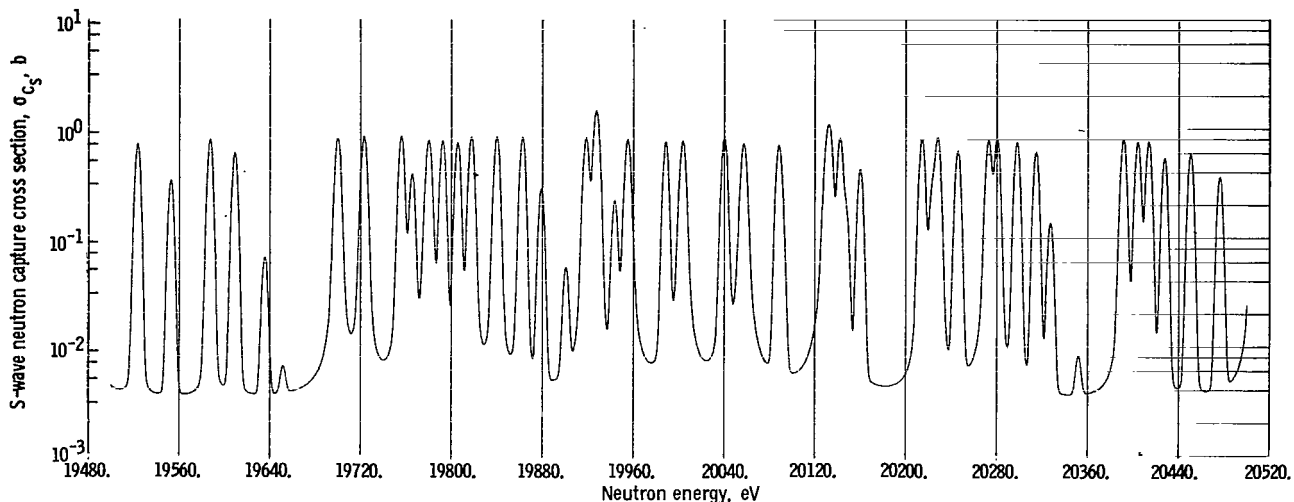


Figure 5. - S-wave capture cross section.

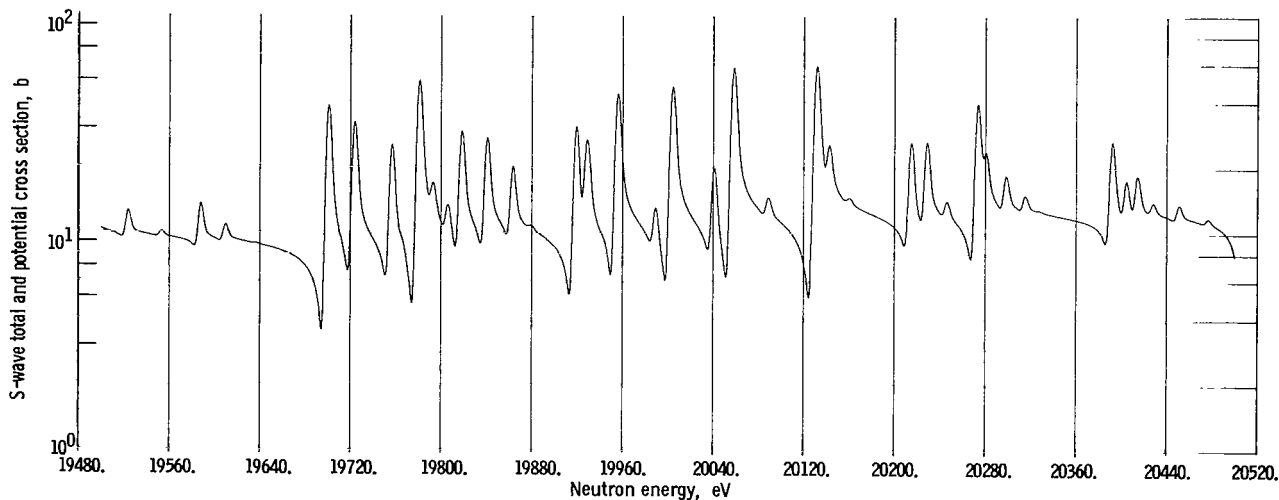


Figure 6. - S-wave total and potential cross section.

The s-wave capture component and the s-wave total cross section showing the scattering interference with the potential cross section about 20 keV are shown in figures 5 and 6. A portion of the p-wave capture cross section and the p-wave total cross section are shown in figures 7 and 8. The total cross section and the total capture cross section are shown in figures 9 and 10. These figures (figs. 5 to 10) show cross sections which have been Doppler broadened to 300 K and have been computed at 0.5-eV intervals.

Table II shows the average values of the cross section components of the average total cross section at 20 keV for an initially selected value of 10.8 barns for the poten-

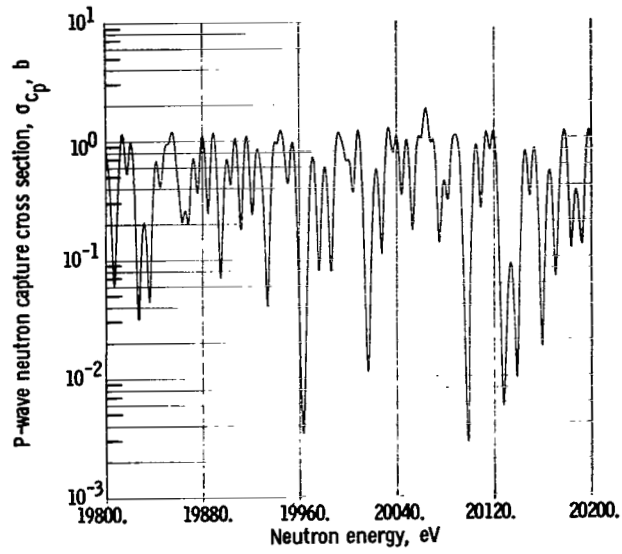


Figure 7. - Portion of p-wave capture cross section.

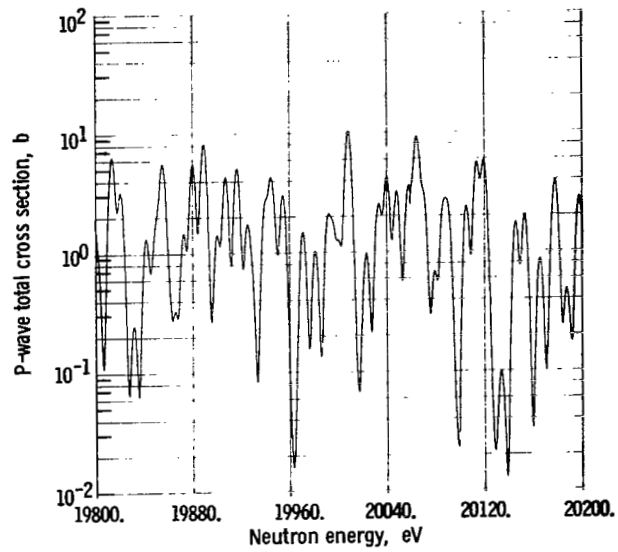


Figure 8. - Portion of p-wave total cross section.

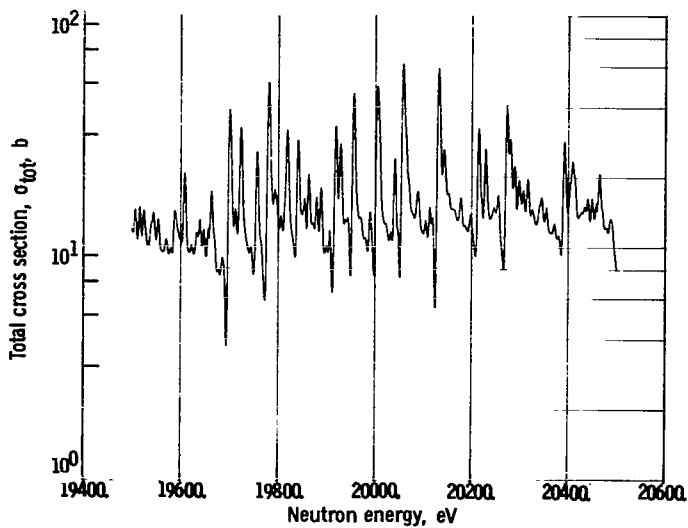


Figure 9. - Total cross section.

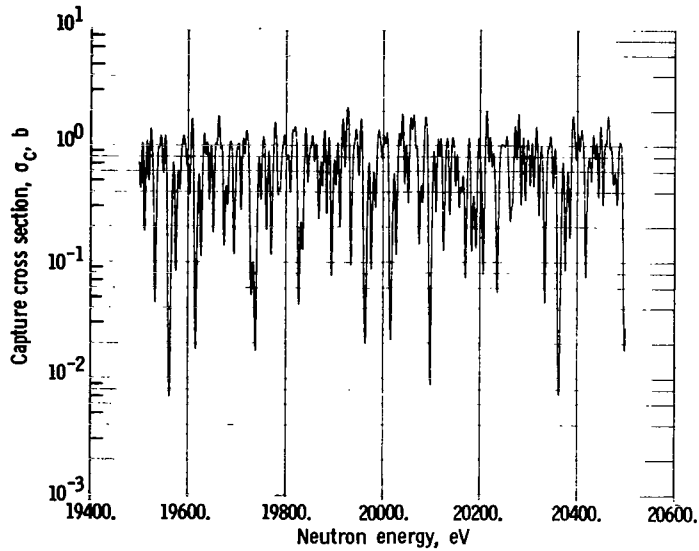


Figure 10. - Total capture cross section.

tial cross section. In column 3 of table II the results of an analytic computation of these averages is shown (ref. 36). This analytic method, that of Lane and Lynn, allows one to accurately compute average cross sections, both s- and p-wave. The results of the DAISY-GAROL computation are in quite good agreement with these analytic results. This agreement indicates the sampling techniques used in DAISY have been implemented correctly. However, according to steps (5) and (6) in the previous section, it is necessary to choose a value of σ_{pot} so as to maintain the measured value of $\bar{\sigma}_{tot}$. The cross

TABLE II. - COMPONENTS OF AVERAGE TOTAL CROSS SECTION FOR U^{238} AT 20 keV BY THE METHOD OF DAISY AND THAT OF LANE AND LYNN (REF. 36)

Component	DAISY	Lane and Lynn (ref. 36)	DAISY (FINAL)
Potential scattering cross section, σ_{pot} , b	10.800	10.800	9.647
Average s-wave scattering cross section, $\bar{\sigma}_{s_s}$, b	2.378	2.381	2.380
Average s-wave capture cross section, $\bar{\sigma}_{c_s}$, b	.165	.163	.165
Average p-wave scattering cross section, $\bar{\sigma}_{s_p}$, b	1.226	1.223	1.074
Average p-wave capture cross section, $\bar{\sigma}_{c_p}$, b	.536	.527	.514
Average total capture cross section, $\bar{\sigma}_c$, b	.701	.690	.679
Average total cross section, $\bar{\sigma}_{\text{tot}}$, b	15.105	15.094	13.780

sections so generated are shown in the last column labeled DAISY (FINAL).

Table III shows three values of the measured average total cross section at 20 keV and three values of the potential cross section inferred as necessary to maintain these three total cross sections (see step (6) in previous section). As it would be extremely difficult to assign any one of these measurements a higher precision than the two others, the average value of σ_{pot} (inferred) equal to 9.647 barns is used for all further calcula-

TABLE III. - VALUES OF σ_{pot} OBTAINED FROM $\bar{\sigma}_{\text{tot}}$ CONSERVATION FROM DIFFERENT SOURCES OF MEASURED CROSS SECTION

Source	$\bar{\sigma}_{\text{tot}}$ (20 keV), b	σ_{pot} (inferred), b
KFK-120 ^a	13.6	9.500
LA-3527 ^b	14.158	9.986
BNL-325 ^c	13.55	9.456
Average inferred potential scattering cross section $\bar{\sigma}_{\text{pot}} = 9.647$		

^aRef. 42.

^bRef. 43.

^cRef. 2.

tions (refs. 37, 38, and 39). The p-wave Γ_n 's have been recomputed using this value of σ_{pot} and equation (15) to obtain the appropriate ν_1 's. The resulting cross section averages from GAROL are shown in table II under the heading DAISY (FINAL).

Graphical Comparisons with Theoretical Distributions

Figures 11 to 16 allow one to compare the individual resonance parameters chosen by DAISY to the theoretical distribution functions. These figures should indicate the detailed resonance structure generated by DAISY in a manner more easily grasped than a table of resonance parameters. The cumulative probability distributions of $\Gamma_n/\bar{\Gamma}_n$ for the s- and p-wave resonance parameters generated by DAISY are shown in figures 11 and 12 along with the theoretical cumulative probability distributions. The cumulative probability distributions of D/\bar{D} for the s- and p-wave resonance energies generated by DAISY are shown in figures 13 and 14 along with cumulative Wigner distribution. It can be seen that the sampled values are in good agreement with the theoretical distributions over their range.

While they are not comparisons of theoretical to sampled data, plots of $N(E)$, the number of levels at or below the energy E , against E are shown for the s- and p-wave chains in figures 15 and 16. These plots serve to indicate the amount of local variation in level spacings.

ANALYSIS OF DOPPLER EFFECT EXPERIMENTS: CALCULATION OF HOT TO COLD CAPTURE RATIOS OF THE $U^{238}(n,\gamma)U^{239}$ REACTION AT 20 keV

The DAISY (FINAL) chain illustrated previously is used solely throughout the remainder of this report. These parameters generated by DAISY allow one to compute a representative shape of the cross section against energy rather than averages alone. In this section the parameters generated by DAISY and the code GAROL (ref. 13) will be used to evaluate the Doppler effect in U^{238} at 20 keV. By the use of the DAISY (FINAL) parameters and GAROL it is possible not only to investigate the effects of resonance series overlap but it is also possible to determine separately the Doppler effect of the s-wave series and p-wave resonance series.

Thin Foil Problem

As a part of a study of the energy and temperature dependence of neutron capture

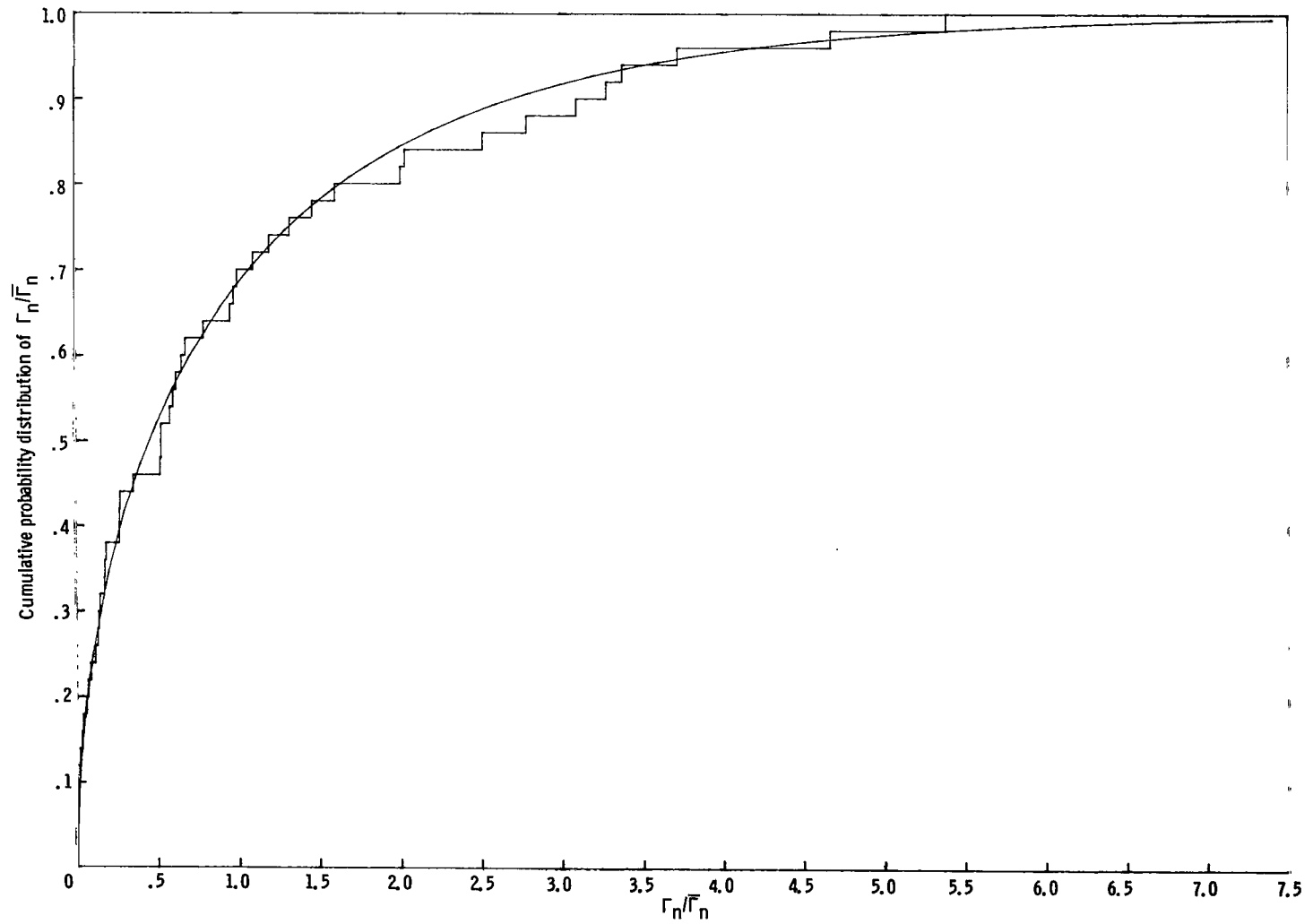


Figure 11. - Cumulative probability distribution of $\Gamma_n/\bar{\Gamma}_n$ compared to that of a χ^2 distribution with one degree of freedom for s-wave DAISY (FINAL) chain.

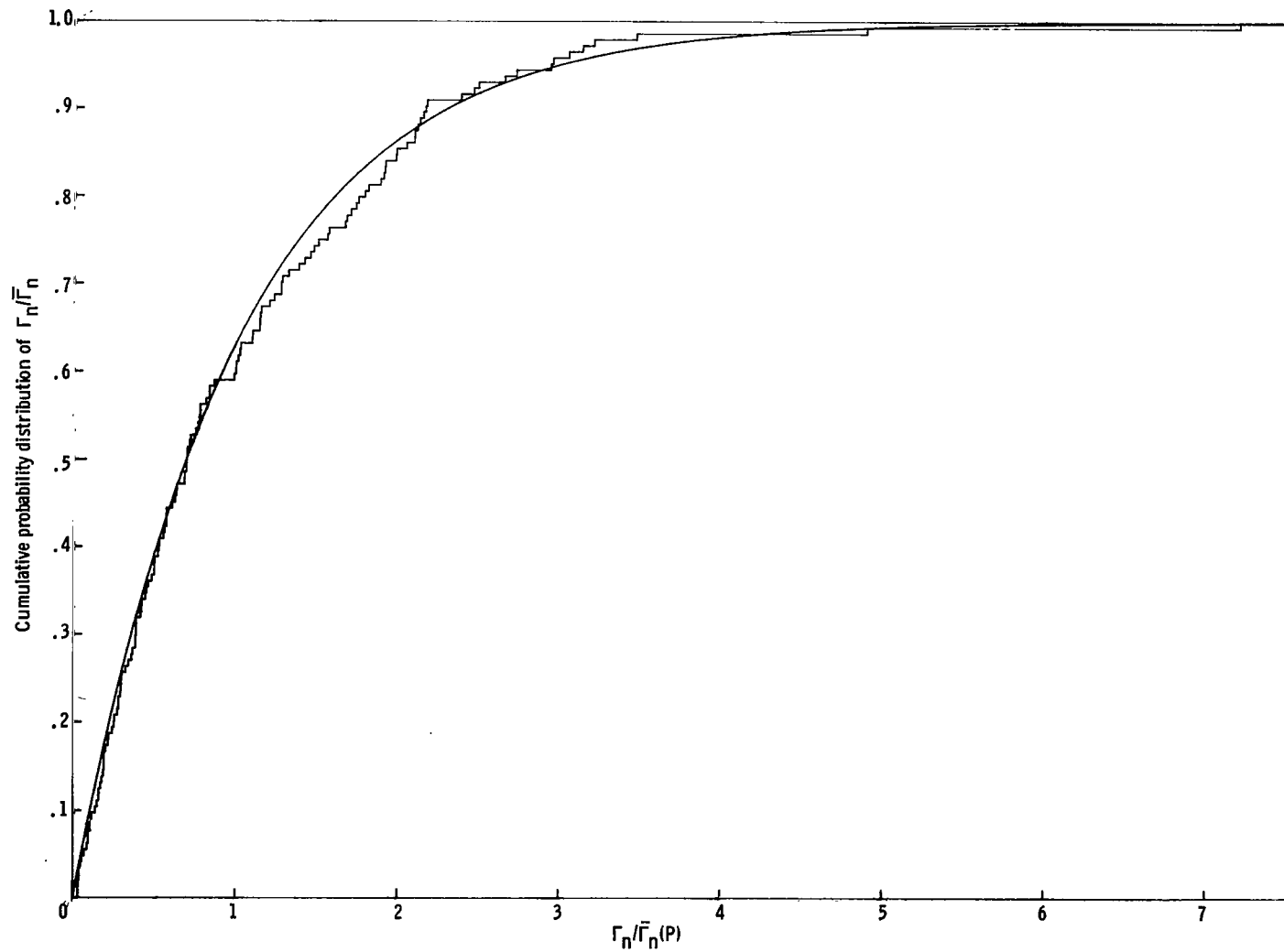


Figure 12. - Cumulative probability distribution of $\Gamma_n/\bar{\Gamma}_n$ compared to that of a χ^2 distribution with two degrees of freedom for p-wave DAISY (FINAL) chain.

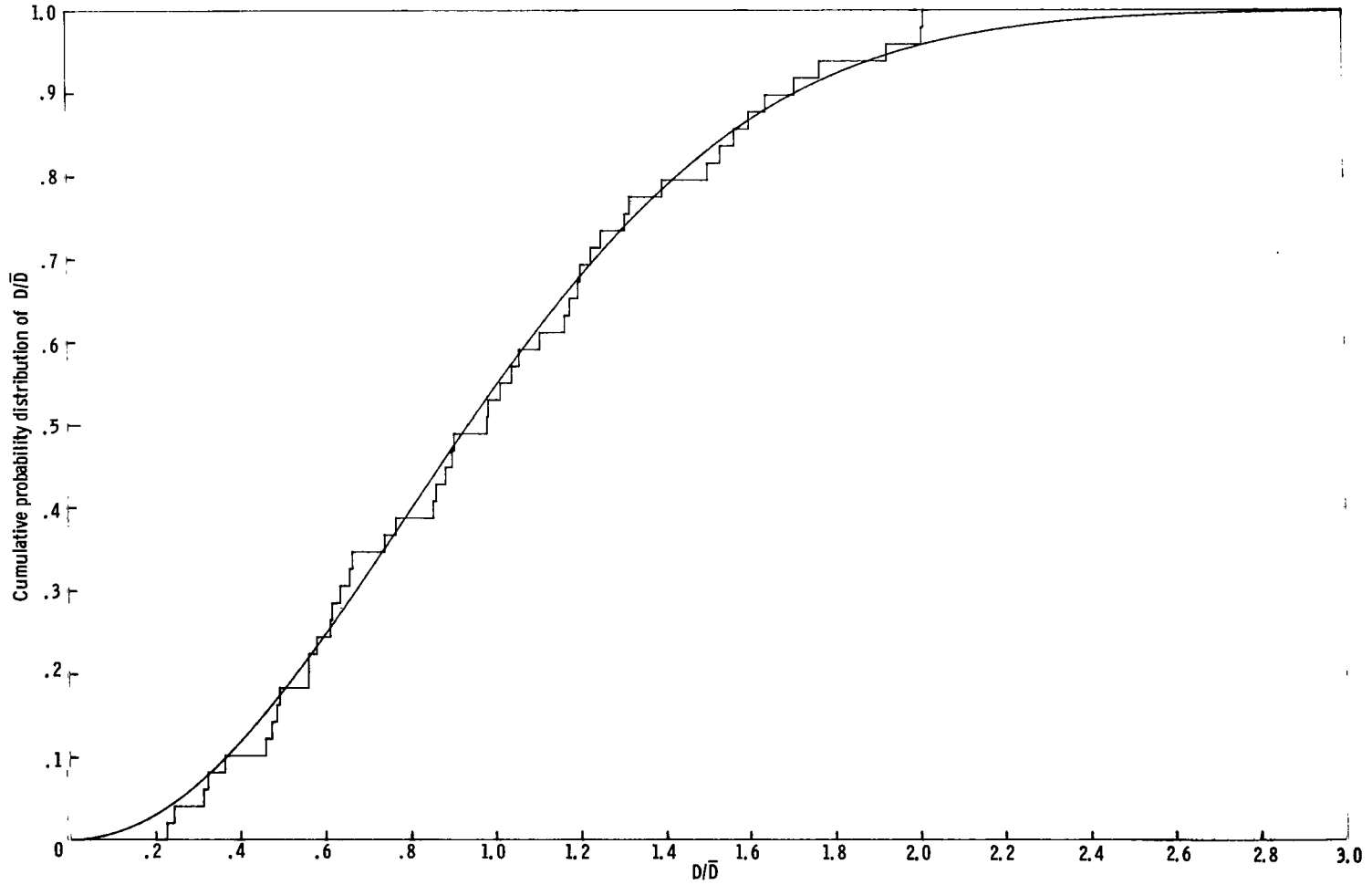


Figure 13. - Cumulative probability distribution of D/\bar{D} compared to the Wigner level spacing distribution for s-wave DAISY (FINAL) chain.

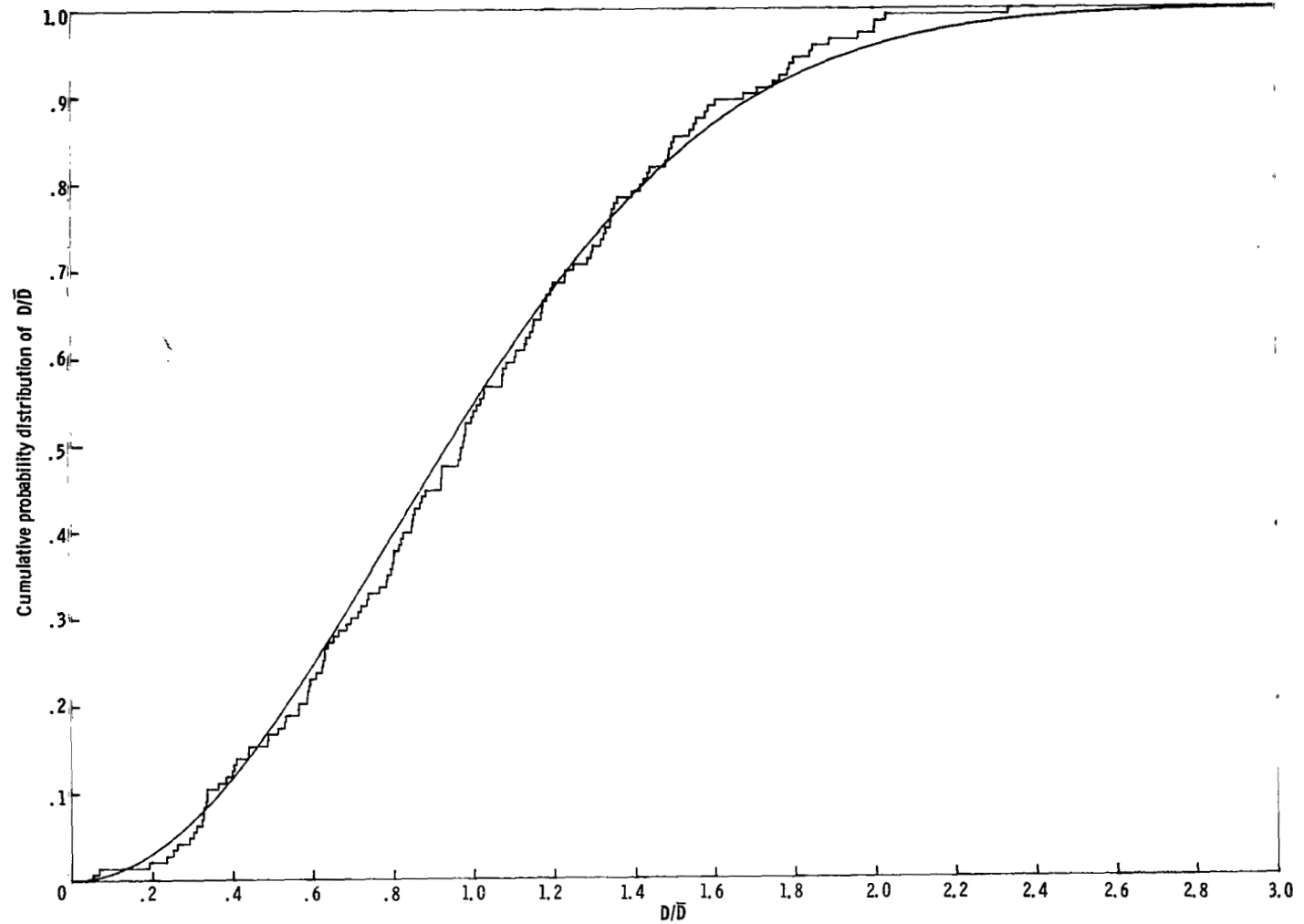


Figure 14. - Cumulative probability distribution of D/\bar{D} compared to the Wigner level spacing distribution for p-wave DAISY (FINAL) chain.

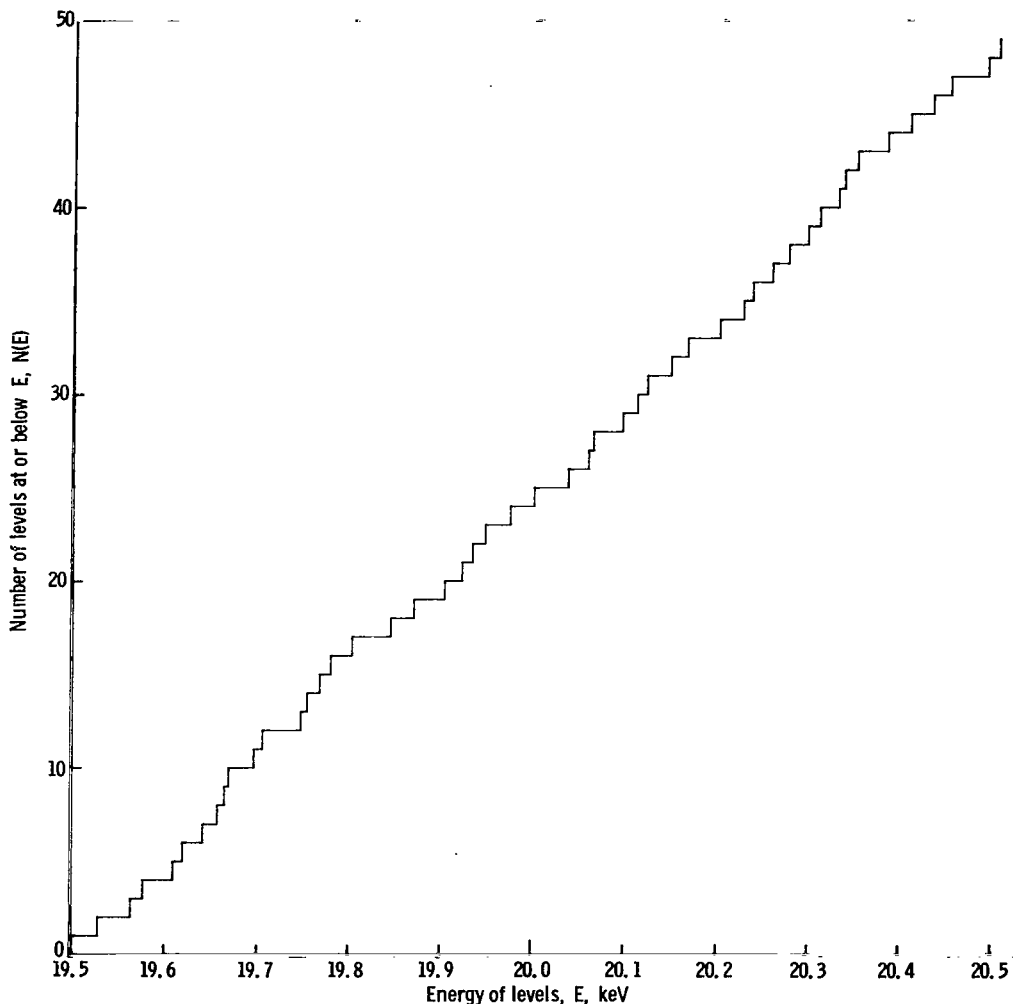


Figure 15. - Number of levels at or below E as a function of energy of levels for s-wave DAISY (FINAL) chain.

measurements in the unresolved region, Seufert and Stegemann (ref. 14) measured the hot and cold neutron capture reaction rates of a U^{238} foil, 0.0155 centimeter thick, in a lead block slowing-down-time neutron energy spectrometer. The temperatures chosen in this experiment were 300 K for the cold sample and 750 K for the hot sample. A theoretical ratio of hot to cold captures is also plotted by Seufert and Stegemann as a function of energy from 300 eV to 30 keV. Their theoretical value of the ratio at 20 keV is 1.0023. No resonance overlap corrections have been applied in their computation of the theoretical hot to cold capture ratio. Unfortunately, the measured ratios in this energy region are subject to rather large error margins. The measured ratio at about 16.5 keV is 1.030 ± 0.024 , and at about 31.5 keV it is 1.019 ± 0.045 . Although experiments are very difficult to perform and experimental results are rather imprecise, it

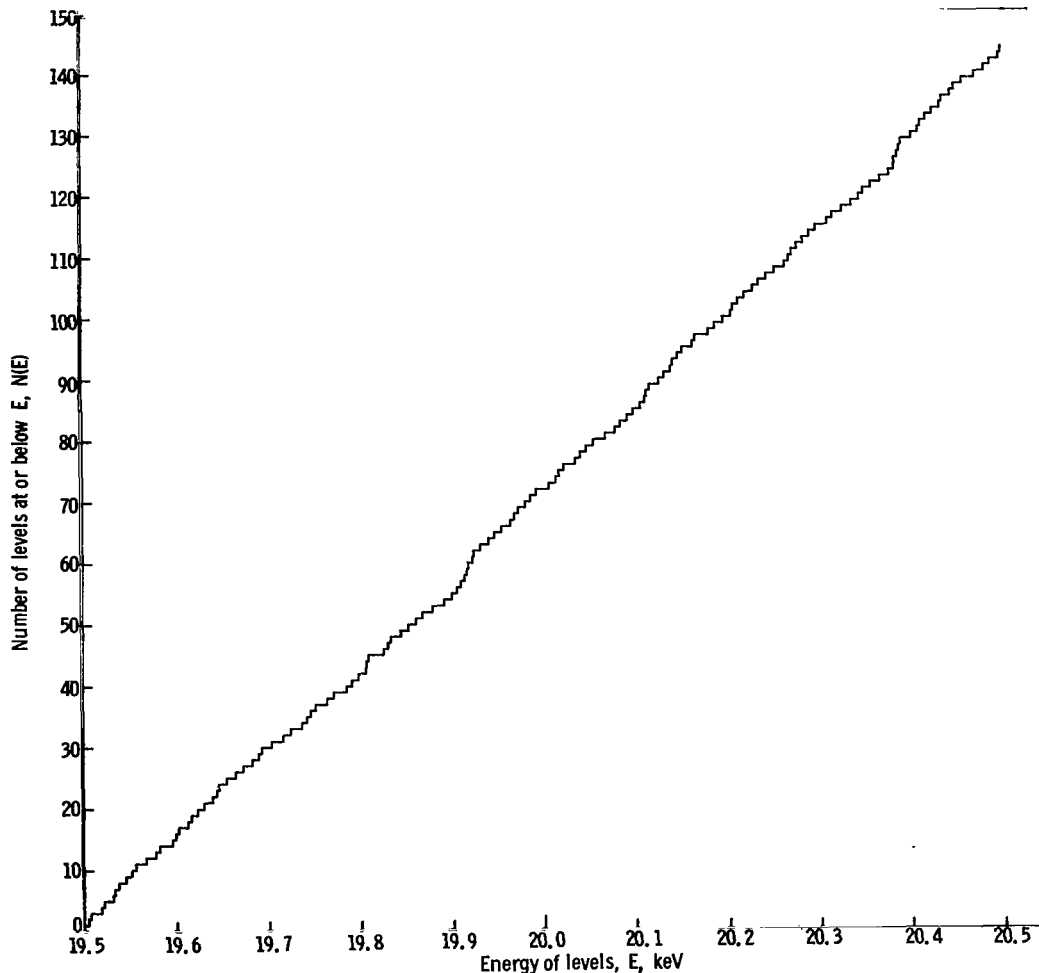


Figure 16. - Number of levels at or below E as a function of energy of levels for p-wave DAISY (FINAL) chain.

is possible to compute the hot to cold reaction ratio, with some precision, in this unresolved resonance region.

The calculation of the hot (750 K) to cold (300 K) ratio for a 0.0155-centimeter-thick slab of U^{238} was made over the interval 19 600 to 20 400 eV by 0.5-eV increments. It is assumed that the slab absorber, the U^{238} foil, is embedded in a purely scattering medium. The results of these calculations are shown in table IV where the hot to cold capture ratios both with and without the overlap effect are displayed.

It can be seen that the DAISY-GAROL calculation of the hot to cold capture ratio without overlap is in substantial agreement with the Seufert and Stegemann calculation which assumes no overlap. The value of the hot to cold capture ratio is reduced from 1.0030 to 1.0023 when resonance series overlap is included. Due to the rather large uncertainty in the experimental results, a direct comparison between theoretical results

TABLE IV. - HOT TO COLD NEUTRON CAPTURE RATIOS

(750 K/300 K) FOR A U^{238} FOIL AT 20-keV

NEUTRON ENERGIES

	Total capture ratio	R_s	R_p
With overlap	1.0023 ± 0.0016	0.0014 -----	0.0009 -----
Without overlap	1.0030 ± 0.0010	.0014 -----	.0016 -----
Seufert and Stegemann theory without overlap ^a	1.0028 -----	-----	-----
Measured at 16.5 keV ^a	1.030 ± 0.024	-----	-----
Measured at 31.5 keV ^a	1.019 ± 0.045	-----	-----

^aRef. 14.

and experiments is precluded. Yet one can determine from the detailed GAROL results the Doppler effects for the separate series. If one assumes that the cold capture rate for the s-wave resonance series is n_s , then the hot capture rate for the s-wave series can be represented by $n_s + \delta n_s$. If the cold and hot capture rates for the p-wave series are represented in the same fashion as n_p and $n_p + \delta n_p$, one can form the hot to cold capture ratio as

$$\frac{n_s + n_p + \delta n_s + \delta n_p}{n_s + n_p} = 1 + \frac{\delta n_s}{n_s + n_p} + \frac{\delta n_p}{n_s + n_p}$$

$$\frac{\delta n_s}{n_s + n_p} = R_s \quad (31)$$

$$\frac{\delta n_p}{n_s + n_p} = R_p \quad (32)$$

The R_s and R_p values are shown for the two cases computed. It should be noted that, while the p-wave average capture cross section is about three times the size of the s-

wave average capture cross section, it (the p-wave resonance series captures) accounts for only about 40 percent of the Doppler effect. Assuming no overlap overestimates the Doppler effect for the p-wave series by about 80 percent. The reason for the rather small p-wave Doppler effect is that the Doppler width for U^{238} at 300 K and 20 000 eV is ~ 3.0 eV. This is over 40 percent of the average p-wave level spacing, 7.0 eV. Thus, the p-wave cross sections are much more nearly smooth than the s-wave cross sections.

The error estimates shown are formed by breaking up the region from 19.6 to 20.4 keV into two regions, one from 19.6 to 20.0 keV and the other from 20.0 to 20.4 keV, computing a capture ratio for each region and then the standard deviation of these two capture ratios is shown below the total capture ratio.

Thick Sphere Problem

Another experiment utilizing a larger temperature variation and thick spheres, 2 centimeters in diameter, has been conducted by Fieldhouse et al. (ref. 12).

The experimental arrangement used the $Li^7(p, n)$ reaction as a source of neutrons. The angle between the proton beam, the target, and the sample to be irradiated as well as the proton beam energy were chosen to obtain the required range of neutron energies on the sample. Two samples of U^{238} were irradiated simultaneously, one sample at room temperature the other at 770 K. At the end of the irradiation, the hot sample was

TABLE V. - HOT TO COLD NEUTRON CAPTURE
RATIOS (770 K/290 K) FOR A U^{238} SPHERE
AT 20-keV NEUTRON ENERGIES

	Total capture ratio	R_s	R_p
With overlap	1.023 ± 0.001	0.013 ----	0.010 ----
Without overlap	1.030 ± 0.001	.013 ----	.017 ----
Theory of Fieldhouse et al. with overlap ^a	1.027 -----	-----	-----
Fieldhouse et al. measured between 10 and 33 keV plotted at 21.5 keV ^a	1.034 ± 0.023	-----	-----

^aRef. 12.

cooled and counted for β activity along with the room temperature sample. Experimental errors were reduced by alternating the temperature in the same furnaces - the 770 K furnace is subsequently run at room temperature (290 K) and the room temperature furnace is subsequently run at 770 K. The results of these experiments are shown in table V. The measured value of the average Doppler effect in the energy region, 10 to 33 keV, plotted at 21.5 keV was 1.034 ± 0.023 (ref. 12).

The Fieldhouse theoretical results used a statistical sampling of resonance parameters and a slowing down code. Therefore, this theoretical result should include s-wave, p-wave series overlap effects explicitly. However, rather different strength functions were used and a potential cross section of 10.636 barns was used in their calculations (refs. 11 and 12). Hence, the DAISY-GAROL results could differ from the theoretical result of Fieldhouse et al., a Doppler effect of 1.027.

The DAISY-GAROL result for the region, 19.6 to 20.4 keV, is 1.023 ± 0.001 including overlap and 1.030 ± 0.001 assuming no s-wave, p-wave series overlap. Thus, there is reasonable agreement between the DAISY-GAROL results and the theoretical result of Fieldhouse et al. Again the p-wave series contribution to the Doppler effect is less than the s-wave, p-wave cross section ratio. There is also an overestimation of the p-wave Doppler effect when resonance series overlap is neglected.

The DAISY-GAROL calculations are done along the same lines as the calculations of reference 12; that is, the U^{238} spheres are assumed to be covered by a thin scattering source of neutrons. For these computations, the source is assumed to be a 0.1-centimeter-thick shell around the 2-centimeter-diameter spheres. The results are not strongly dependent upon the thickness of this shell. When these calculations are repeated for a shell with an optical thickness of 100 000.0 centimeters, the Doppler effect, including overlap, is raised to only 1.046.

SUMMARY OF RESULTS

Using only one set of resonance parameters, determined by the code DAISY, one can not only match total cross sections in the unresolved energy region but one can also compute Doppler effects, compatible with other theoretical calculations, over a wide range of sample thicknesses (0.0155 to 2 cm).

The results obtained are as follows:

1. The techniques used in the code DAISY allow one to efficiently choose a pseudo resonance parameter chain consistent with the Porter-Thomas and Wigner distribution functions.

2. The cross section averages computed by the DAISY-GAROL combination are in very good agreement with averages computed by analytic techniques.

3. A value of about 9.6 ± 0.3 barns is necessary for the potential cross section in these calculations to preserve the measured value of the total cross section of U^{238} at 20 keV.

4. By the use of one set of parameters, DAISY (FINAL), and the code GAROL, one may compute the Doppler effect at 20 keV.

5. The Doppler effects computed by the DAISY-GAROL combination are compatible with other theoretical computations of the Doppler effect over a wide range of thicknesses (0.0155 to 2 cm).

6. The effect of neglecting resonance series overlap is to overestimate the Doppler effect.

7. The s-wave contribution to the Doppler effect is from 50 to 60 percent, but the average s-wave capture cross section is about one-third that of the p-wave capture cross section.

In conclusion, a technique for the rapid generation of resonance parameter chains in the unresolved resonance region has been described and used in conjunction with a standard nuclear code to evaluate Doppler effects in U^{238} .

Lewis Research Center,
National Aeronautics and Space Administration,
Cleveland, Ohio, April 1, 1970,
129-02.

APPENDIX A

SAMPLING FROM A χ^2 DISTRIBUTION

The purpose of this appendix is to prove that sampling ν times from a normal distribution, squaring the samples and summing provides a χ^2 sample of ν degrees of freedom.

First, $M_x(\theta)$, the moment generating function of $f(x)$ is defined as follows:

$$M_x(\theta) = \int_{-\infty}^{\infty} e^{\theta x} f(x) dx$$

Also, it can be shown (refs. 29, 30, and 40) that, if two random variables have the same moment generating function, they are identical.

Next, the moment generating function of the χ^2 distribution with ν degrees of freedom shall be computed as follows:

$$M_{\chi^2}(\theta) = \frac{1}{2^{\nu/2} \Gamma\left(\frac{\nu}{2}\right)} \int_0^{\infty} e^{\theta x^2} (\chi^2)^{(\nu-2)/2} e^{-\chi^2/2} d(\chi^2)$$

If χ^2 is replaced by w , the result is

$$M_w(\theta) = \frac{1}{2^{\nu/2} \Gamma\left(\frac{\nu}{2}\right)} \int_0^{\infty} e^{\theta w} w^{(\nu-2)/2} e^{-w/2} dw$$

If $z = w(1 - 2\theta)/2$ $dw = 2 dz/(1 - 2\theta)$,

$$M_w(\theta) = \frac{(1 - 2\theta)^{-\nu/2}}{\Gamma\left(\frac{\nu}{2}\right)} \int_0^{\infty} e^{-z} z^{(\nu/2)-1} dz$$

$$M_w(\theta) = \frac{(1 - 2\theta)^{-\nu/2}}{\Gamma\left(\frac{\nu}{2}\right)} \Gamma\left(\frac{\nu}{2}\right)$$

$$M_w(\theta) = (1 - 2\theta)^{-\nu/2}$$

$$M_{\chi^2}(\theta) = (1 - 2\theta)^{-\nu/2}$$

Now the moment generating function of the sum of the squares of samples chosen from the normal distribution function will be determined. Use will be made of the following theorem (refs. 29, 30, and 40). The moment generating function of the sum of n independent random variables is equal to the product of the moment generating functions of the individual variables. If x is normally distributed with mean 0 and variance 1, let a random sample of ν values of x_i be taken from the distribution. Now the moment generating function of q shall be computed. Where

$$q = \sum_{i=1}^{\nu} x_i^2$$

$$M_q(\theta) = M_{x_1^2 + \dots + x_\nu^2}(\theta) = M_{x_1^2}(\theta) \cdot M_{x_2^2}(\theta) \cdot \dots \cdot M_{x_\nu^2}(\theta) = \left[M_{x^2}(\theta) \right]^\nu$$

Since x is normally distributed,

$$M_{x^2}(\theta) = \frac{1}{\sqrt{2\pi}} \int_{-\infty}^{\infty} e^{\theta x^2} e^{-x^2/2} dx$$

Let $y = x(1 - 2\theta)^{1/2}$; then

$$M_{x^2}(\theta) = (1 - 2\theta)^{-1/2} \frac{1}{\sqrt{2\pi}} \int_{-\infty}^{\infty} e^{-y^2/2} dy = (1 - 2\theta)^{-1/2}$$

Recalling the previous result gives

$$M_q(\theta) = \left[M_{x^2}(\theta) \right]^\nu = \left[(1 - 2\theta)^{-1/2} \right]^\nu = (1 - 2\theta)^{-\nu/2}$$

which is exactly the same result as the generating function of χ^2 with ν degrees of freedom.

Thus, since the moment generating functions are equal, the distribution functions are identical. If one wishes to sample from a χ^2 distribution with ν degrees of freedom, one needs only to sample the normal distribution ν times, square the results, and sum.

APPENDIX B

FAST GENERATOR FOR NORMAL RANDOM VARIABLES

It has been shown that, if one wishes to sample from the χ^2 distribution with ν degrees of freedom, the problem may be reduced to sampling from the normal distribution. The purpose of this appendix is to outline in some detail a fast procedure (ref. 23) for sampling the normal distribution.

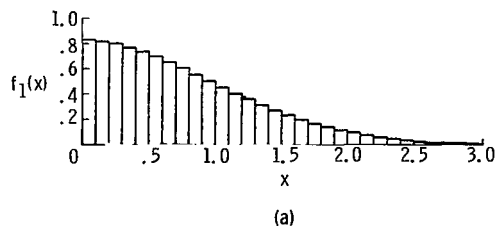
The procedure is most simply explained as follows. The density function $f(x)$ of the positive normal distribution is divided into three portions

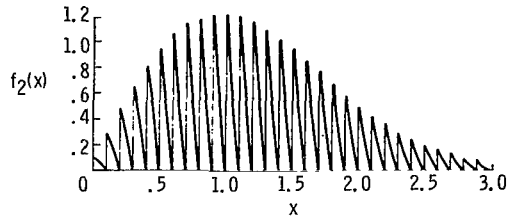
$$f(x) = \frac{\sqrt{2} e^{-1/2x^2}}{\sqrt{\pi}} = 0.9578 f_1(x) + 0.0395 f_2(x) + 0.0027 f_3(x)$$

The meaning of this formula is that one generates, with probability 0.9578 a random variable with density f_1 , with probability 0.0395 a random variable with density f_2 , and finally with probability 0.0027 a random variable with density f_3 . The exact probabilities can be determined from reference 23. The importance of this splitting of the density function is that the procedure which gives f_1 is extremely fast, the procedure for f_2 is rather short, and the time for f_3 rather long.

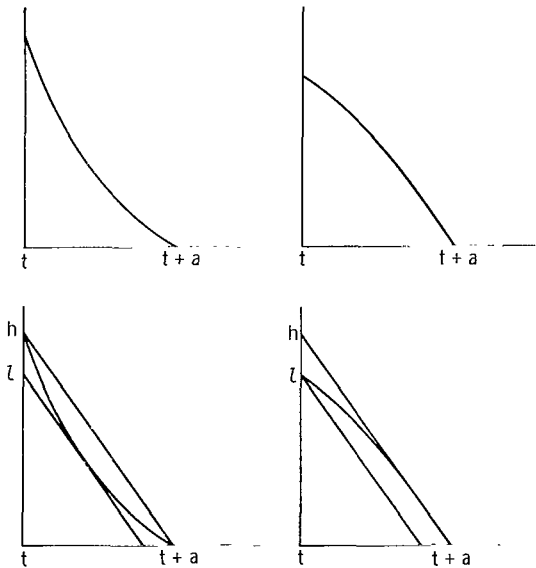
The procedure for f_1 depends upon representing much of the area under the density curve $f(x)$ as a series of uniformly distributed random variables with differing probabilities of being chosen (sketch (a)). A stored series of values then allows the use of the first few digits of a uniformly distributed random number to choose the correct leading digits of the variate f_1 and the rest of the uniform random variable gives the rest of f_1 . If the stored values are contained in the vector A_i and if the uniformly distributed random variable u has digits $0 \cdot u_1, u_2, u_3, \dots, u_7$. If $00 \leq u_1 u_2 \leq 79$, put the normal random variable $x = A_{u_1 u_2} + \cdot 0 u_4 u_5 u_6 u_7$.

If $790 \leq u_1 u_2 u_3 < 940$, put $x = A_{u_1 u_2 u_3} - 771 + \cdot 0 u_4 u_5 u_6 u_7$. This will generate the variable shown in sketch (a). In order to generate the correct random variable $f(x)$ in the range $0 \leq x < 3.0$, a sample must also be taken from the density function $f_2(x)$





(b)



(c)

shown in sketch (b) with probability 0.0395. This is accomplished by a modified rejection technique. It can be shown for a nearly linear density function, as is shown in sketch (c), that the following technique will provide a correct sampling (ref. 41). In order to generate a random variable Y from a nearly linear density function $g(x)$ for $t < x < t + a$, first contain $g(x)$ within two parallel lines. Then choose two independent random variables u and v distributed uniformly on the unit interval $(0, 1)$. If the larger of u and v is less than l/h , set $Y = t + a \min(u, v)$. If the larger of u and v is not less than l/h , then find out if

$$h|u - v| < g[t + a \min(u, v)]$$

If true, put $Y = t + a \min(u, v)$; otherwise generate a new u and v and start this entire procedure again.

The two techniques described previously allow one to generate the correct density

function for the normal distribution to a value of the random variable of 3.0. Beyond 3.0 a process which is executed for only 0.27 percent of the values. It is a modification of a technique found in reference 25 and shall not be described inasmuch as it does not affect the timing a great deal. The interested reader is referred to references 23 and 25.

The aforementioned procedures including the one not described in detail have been programmed in a FORTRAN IV subroutine. It provides on the order of 5000 normal random variables per second on the Lewis 7094-II.

REFERENCES

1. Glass, N. W.; Schelberg, A. D.; Tatro, L. D.; and Warren, J. H.: ^{238}U Neutron Capture Results from Bomb Source Neutrons. Proceedings of the Second Conference on Neutron Cross Sections and Technology. D. T. Goldman, ed. Spec. Publ. 299, vol. 1, National Bureau of Standards, 1968, pp. 573-587.
2. Stehn, John R.; et al.: Neutron Cross Sections. Vol. III, Z = 88 to 98. Rep. BNL-325, 2nd ed., suppl. 2, vol. III, Brookhaven National Lab., Feb. 1965, pp. 92-238-24 to 92-238-25.
3. Greebler, P.; Hurwitz, H., Jr.; and Storm, M. L.: Statistical Evaluation of Fission-Product Absorption Cross Sections at Intermediate and High Energies. Nucl. Sci. Eng., vol. 2, no. 3, May 1957, pp. 334-351.
4. Gordeev, I. V.; and Pupko, V. Y.: Evaluation of the Absorption Cross Section of U^{235} Fission Fragments in the Energy Range 0.025 eV to 1 Mev and Calculation of Fragment Effects in Intermediate Reactors. Nuclear Data and Reactor Theory. Vol. 16 of Proceedings of the Second United Nations International Conference on the Peaceful Uses of Atomic Energy. United Nations, 1958, pp. 141-149.
5. Garrison, J. D.; and Roos, B. W.: Fission-Product Capture Cross Sections. Nucl. Sci. Eng., vol. 12, no. 1, Jan. 1962, pp. 115-134.
6. Brissenden, R. J.; and Durston, C.: The Calculation of Neutron Spectra in the Doppler Region. Proceeding of the Conference on the Application of Computing Methods to Reactor Problems. Rep. ANL-7050, Argonne National Lab., 1965, pp. 51-76.
7. Moore, M. S.; and Simpson, O. D.: Measurement and Analysis of Cross Sections of Fissile Nuclides. Conferences on Neutron Cross Section Technology. AEC Rep. CONF-660303, Book 2, 1966, pp. 840-872.
8. Bogart, Donald; and Semler, Thor T.: Monte Carlo Interpretation of Sphere Transmission Experiments for Average Capture Cross Sections at 24 keV. Neutron Cross Section Technology. AEC Rep. CONF-660303, Book 1, 1966, pp. 502-521.
9. Dyos, M. W.: Construction of Statistical Resonances in the Unresolved Resonance Region: The PSEUDO Code. Rep. GA-7136, General Dynamics Corp., May 26, 1966.
10. Lowery, Virgil W.; and Sakolosky, George P., eds.: Progress in Reactor Physics. AEC Rep. WASH-1125, Jan. 1969, pp. 7-8, 23.

11. Perkin, J. L.; Fieldhouse, P.; Brickstock, A.; and Davies, A. R.: Measurements and Calculations of the Doppler Effect on the Reactions $^{238}\text{U}(n, \gamma)$, $^{235}\text{U}(n, f)$ and $^{239}\text{Pu}(n, f)$ with Neutrons in the Energy Range 0-25 keV. J. Nucl. Energy, Pts. A/B, vol. 20, no. 11/12, 1966, pp. 921-937.
12. Fieldhouse, P.; et al.: The Doppler Effect on the $^{238}\text{U}(n, \gamma)$ Reaction at Different Neutron Energies and at High Temperatures. J. Nucl. Energy, vol. 21, no. 11, 1967, pp. 847-855.
13. Stevens, C. A.; and Smith, C. V.: GAROL: A Computer Program for Evaluating Resonance Absorption Including Resonance Overlap. Rep. GA-6637, General Dynamics Corp. (NASA CR-71162), Aug. 24, 1965.
14. Seufert, H.; and Stegemann, D.: Energy and Temperature Dependent Capture Measurements Below 30 keV Supporting Doppler Effect Calculations. Rep. KFK-631, Kernforschungsanlage, Karlsruhe, Oct. 1967.
15. Porter, C. E.; and Thomas, R. G.: Fluctuations of Nuclear Reaction Widths. Phys. Rev., vol. 104, no. 2, Oct. 15, 1956, pp. 483-491.
16. Wigner, E. P.: Results and Theory of Resonance Absorption. Conference on Neutron Physics by Time-of-Flight, Gatlinburg, Tenn., Nov. 1-2, 1956. Rep. ORNL-2309, Oak Ridge National Lab., 1957, pp. 59-70.
17. Gaudin, Michel: Sur La Loi Limite De L'Espacement Des Valeurs Propres D'Une Matrice Aléatoire. Nucl. Phys., vol. 25, 1961, pp. 447-458.
18. Desjardins, J. S.; Rosen, J. L.; Havens, W. W., Jr.; and Rainwater, J.: Slow Neutron Resonance Spectroscopy. II. Ag, Au, Ta. Phys. Rev., vol. 120, no. 6, Dec. 15, 1960, pp. 2214-2226.
19. Julien, J.; et al.: Détermination Du Spin Et Des Paramètres Des Résonances Pour $^{197}\text{Au} + n$ de 10 eV a 1000 eV. Nucl. Phys., vol. 76, 1966, pp. 391-432.
20. Garg, J. B.; Rainwater, J.; Petersen, J. S.; and Havens, W. W., Jr.: Neutron Resonance Spectroscopy. III. Th 232 and U 238 . Phys. Rev., vol. 134, no. 5B, June 8, 1964, pp. 985-1009.
21. Preston, Melvin A.: Physics of the Nucleus. Addison-Wesley Publ. Co., Inc., 1962, pp. 505-508.
22. Fricke, M. P.; and Lopez, W. M.: Radiative Strength Function for Fast Neutron Capture. Phys. Letters, vol. 29B, no. 7, June 23, 1969, pp. 393-395.
23. Marsaglia, G.; MacLaren, M. D.; and Bray, T. A.: A Fast Procedure for Generating Normal Random Variables. Comm. ACM, vol. 7, no. 1, Jan. 1964, pp. 4-10.

24. Cameron, A. G. W.; Lazor, N. H.; and Schmitt, H. W.: Fast Neutron Capture Cross Sections. Fast Neutron Physics. Vol. 2. J. B. Marion and J. L. Fowler, eds., Interscience Publishers, 1963, pp. 1748-1750.
25. Parzen, Emanuel: Modern Probability Theory and Its Applications. John Wiley & Sons, Inc., 1960.
26. Abramowitz, Milton; and Stegun, Irene A., eds.: Handbook of Mathematical Functions with Formulas, Graphs, and Mathematical Tables. Appl. Math. Series no. 55, National Bureau of Standards, second printing, Nov. 1964.
27. Lindgren, Bernard W.; and McElrath, G. W.: Introduction to Probability and Statistics. Macmillan Co., 1959, pp. 154-158.
28. Hald, Anders: Statistical Theory with Engineering Applications. John Wiley & Sons, Inc., 1952, pp. 739-741.
29. Arley, Niels; and Buch, K. Rander: Introduction to the Theory of Probability and Statistics. John Wiley & Sons, Inc., 1950.
30. Cramer, Harold: Mathematical Methods of Statistics. Seventh ed., Princeton University Press, 1957.
31. Firk, F. W. K.; Lynn, J. E.; and Moxon, M. C.: Resonance Parameters of the Neutron Cross Section of U^{238} . Nucl. Phys., vol. 41, 1963, pp. 614-629.
32. Seth, K. K.; Tabony, R. H.; Bilpuch, E. G.; and Newson, H. W.: s-, p-, and d-Wave Neutron Strength Functions. Phys. Letters, vol. 13, no. 1, Nov. 1, 1964, pp. 70-72.
33. Asghar, M.; Chaffey, C. M.; and Moxon, M. C.: Low-Energy Neutron Resonance Parameters of ^{238}U . Nucl. Phys., vol. 85, 1966, pp. 305-316.
34. Uttley, C. A.; Newstead, C. M.; and Diment, K. M.: Neutron Strength Function Measurements in the Medium and Heavy Nuclei. IAEA Conference Proceedings on Nuclear Data for Reactors. AEC Rep. CONF-661014, vol. 1, 1967, pp. 165-174.
35. Anon.: CINDA 67 - An Index to the Literature on Microscopic Neutron Data, Part I. USAEC, Division of Technical Information Extension, TID-24049, 1967, p. 679.
36. Lane, A. M.; and Lynn, J. E.: Fast Neutron Capture Below 1 MeV: The Cross Sections for ^{238}U and ^{232}Th . Proc. Phys. Soc., (London), Sec. A, vol. 70, pt. 8, Aug. 1957, pp. 557-570.
37. Semler, Thor T.: Analysis of Gold Sphere Transmission Experiments at 24-keV Neutron Energy Using Spin-Dependent s-Wave Statistics. NASA TN D-5211, 1969.

38. Miller, L. B.; and Poenitz, W. P.: Monte Carlo Interpretation of a ^{238}U Spherical Shell Transmission Experiment at 23 keV. Nucl. Sci. Eng., vol. 35, no. 2, Feb. 1969, pp. 295-297.
39. McKee, R. J.: μ -Atomic Hyperfine Structure in the K, L, and M Lines of U^{238} and Th^{232} . Phys. Rev., vol. 180, no. 4, Apr. 20, 1969, pp. 1139-1158.
40. Hoel, Paul G.: Introduction to Mathematical Statistics. Second ed., John Wiley & Sons, Inc., 1954.
41. Kahn, Herman: Applications of Monte Carlo. Rep. RM-1237-AEC, Rand Corp. (AEC Rep. AECU-3259), Apr. 19, 1954.
42. Schmidt, J. J.: Neutron Cross Sections for Fast Reactor Materials. Part III. Graphs. Rep. KFK-120, Pt. III, Kernforschungszentrum, Karlsruhe, Dec. 1962, p. 225.
43. Berlijn, J.-J. H.; Hunter, R. E.; and Cremer, C. C.: Neutron Cross Sections for ^{235}U and ^{238}U in the Energy Range 1 keV to 14 MeV. Rep. LA-3527, Los Alamos Scientific Lab., Aug. 1968.

NATIONAL AERONAUTICS AND SPACE ADMINISTRATION
WASHINGTON, D. C. 20546
OFFICIAL BUSINESS

FIRST CLASS MAIL



POSTAGE AND FEES PAID
NATIONAL AERONAUTICS &
SPACE ADMINISTRATION

040 001 49 51 305 70134 00903
WALLACE W. RABBITTS LABORATORY /ALC/L/
KILGORE AVENUE, NEW MEXICO 87117

ATTENTION: WALLACE W. RABBITTS, ALC/L, ARMY

POSTMASTER: If Undeliverable (Section 1103, Postal Manual) Do Not Ret

"The aeronautical and space activities of the United States shall be conducted so as to contribute . . . to the expansion of human knowledge of phenomena in the atmosphere and space. The Administration shall provide for the widest practicable and appropriate dissemination of information concerning its activities and the results thereof."

— NATIONAL AERONAUTICS AND SPACE ACT OF 1958

NASA SCIENTIFIC AND TECHNICAL PUBLICATIONS

TECHNICAL REPORTS: Scientific and technical information considered important, complete, and a lasting contribution to existing knowledge.

TECHNICAL NOTES: Information less broad in scope but nevertheless of importance as a contribution to existing knowledge.

TECHNICAL MEMORANDUMS: Information receiving limited distribution because of preliminary data, security classification, or other reasons.

CONTRACTOR REPORTS: Scientific and technical information generated under a NASA contract or grant and considered an important contribution to existing knowledge.

TECHNICAL TRANSLATIONS: Information published in a foreign language considered to merit NASA distribution in English.

SPECIAL PUBLICATIONS: Information derived from or of value to NASA activities. Publications include conference proceedings, monographs, data compilations, handbooks, sourcebooks, and special bibliographies.

TECHNOLOGY UTILIZATION PUBLICATIONS: Information on technology used by NASA that may be of particular interest in commercial and other non-aerospace applications. Publications include Tech Briefs, Technology Utilization Reports and Notes, and Technology Surveys.

Details on the availability of these publications may be obtained from:

SCIENTIFIC AND TECHNICAL INFORMATION DIVISION
NATIONAL AERONAUTICS AND SPACE ADMINISTRATION
Washington, D.C. 20546